JOURNAL OF
EMERGING INVESTIGATORS

Article

Variation, relationship, and trade-offs of leaf traits in large and small deciduous broadleaf tree species

Tongfei Yan[1,2], Daiyue Pan[3], Shanshan Jin[4]
[1] Rock Bridge High School, Columbia, Missouri
[2] Zhengzhou No.7 Senior High School, Zhengzhou, Henan, China
[3] Zhengzhou No.4 Senior High School, Zhengzhou, Henan, China
[4] College of Forestry, Henan Agricultural University, Zhengzhou, Henan, China

SUMMARY

Leaf traits serve as indicators of plant responses to environmental changes and play a pivotal role in shaping ecosystem functions. Deciduous broadleaf trees, widely planted in temperate urban forests, contribute significantly to carbon cycling, water regulation, and biodiversity. Their sensitivity to shifts in temperature and precipitation makes them useful indicators of ecological change. Leaf traits such as nutrient content, specific leaf area, and water-use efficiency are especially informative, as they reflect physiological responses and adaptive strategies under changing conditions. We hypothesized that large and small deciduous broadleaf tree species would exhibit significant differences in variation, relationships, and trade-offs between leaf traits. By examining 12 key structural, chemical, and photosynthetic leaf traits across 10 representative tree species in Zhengzhou, China, we aimed to uncover the patterns and interconnections underlying these traits. The results showed significant differences in key leaf functional traits between large and small tree species. Specifically, large trees had greater leaf area, equivalent water thickness, and leaf phosphorus content than small species, suggesting an emphasis on resource conservation. In contrast, small trees exhibited higher specific leaf area, leaf nitrogen-to-phosphorus ratio, and photosynthetic rates than big species, reflecting a fast-growth strategy. For small trees, leaf dry matter content was positively related to photosynthetic parameters, further suggesting their rapid resource acquisition, while large trees favored traits supporting resource retention and stress tolerance. This study highlights the heterogeneity and adaptive mechanisms of leaf functional traits in different tree species, offering valuable insights into plant configuration and climate adaptation management strategies.

INTRODUCTION

Under the influence of global climate change, the variation, relationships, and trade-offs of plant functional traits have emerged as critical areas of research. Plant functional traits are not only highly adaptive to environmental changes but also exhibit significant plasticity, making them essential indicators for assessing plant responses to varying ecological conditions (1, 2). In recent years, quantitative analyses of these traits have provided insights into the mechanisms underlying trait variation and resource allocation strategies, enhancing our understanding of plant-environment interactions. For example, leaf area (LA) and plant height have been shown to strongly influence above-ground net primary productivity, underscoring the role of functional traits in regulating ecosystem processes under changing conditions (3). In addition, environmental drivers such as precipitation and temperature significantly affect leaf structural traits, including leaf thickness and specific leaf area (SLA), and chemical traits, including leaf nitrogen content (LNC), leaf phosphorus content (LPC), and leaf carbon content (LCC), thereby influencing plant resource use strategies and adaptation to climatic variability (4).

Leaves, the primary sites for photosynthesis, respiration, and transpiration, play a pivotal role in tree growth, development, and adaptability. Over evolutionary timescales, leaf traits have shown sensitivity to environmental changes and exhibit remarkable phenotypic plasticity (5). For instance, seedling relative growth rate is consistently associated with key traits such as LNC and SLA (5). Additionally, one study analyzed data from 474 species spanning eight growth forms and found that continuous leaf traits (e.g., SLA, LNC) are more reliable predictors of plant responses to nutrient availability than growth form (6).

Although substantial progress has been made in studying leaf structural traits, less attention has been paid to photosynthetic physiological traits, which are critical indicators of plant growth potential and stress tolerance. For instance, the net photosynthetic rate (P_n), which represents the rate at which plants convert carbon dioxide into organic compounds through photosynthesis, directly influences carbon assimilation efficiency (7). Meanwhile, stomatal conductance (G_s), which measures the rate of gas exchange through leaf stomata, reflects both water-use efficiency and a plant's ability to tolerate drought conditions (7). Similarly, intercellular CO_2 concentration (*C*i) reveals the balance between CO_2 assimilation and stomatal behavior (7). The interplay between structural traits and photosynthetic efficiency is equally significant; for example, plants may optimize light capture and carbon assimilation by increasing leaf area while reducing water loss through changes in leaf morphology (8).

Systematic investigations into variation patterns and trade-offs of leaf traits are essential for understanding plant ecological strategy such as resource acquisition, conservation, and stress tolerance under climate change (9). While structural traits such as SLA and LA are well studied, the variability and interrelationships of photosynthetic physiological traits, especially across different plant growth forms—trees, shrubs, and herbaceous plants—remain poorly understood (2,9-11). These traits not only influence morphological and ecological functions (e.g., leaf shape, size, competition, habitat structuring) but also provide critical

https://doi.org/10.59720/25-029

insights into plant adaptation and responses to environmental change (12).

In this study, we hypothesized that significant differences exist in the variation, relationships, and trade-offs of leaf traits between large and small deciduous broadleaf tree species, classified based on height and diameter at breast height (DBH). Larger tree species typically allocate resources toward long-term growth and survival, which may manifest in leaf traits that favor resource conservation, such as lower SLA and higher leaf dry matter content (LDMC) (13). Conversely, small tree species, which prioritize rapid growth and reproduction, are likely to display leaf traits that facilitate higher photosynthetic efficiency and greater nutrient turnover (13). These differing strategies are hypothesized to result in distinct interrelationships among leaf traits and varying trade-offs between growth and resource conservation (14). To test this hypothesis, we measured 12 functional traits encompassing structural, chemical, and photosynthetic parameters to investigate their variation patterns and interrelationships across 10 representative large and small deciduous broadleaf tree species in Zhengzhou, China. Our findings revealed significant variation across traits: large trees exhibited higher LA, equivalent water thickness, and LPC, indicative of resource conservation strategies. In contrast, small trees displayed higher SLA, LNC, leaf nitrogen to phosphorus ratio (leaf N:P), and photosynthetic traits. Distinct scaling relationships were observed, including a positive correlation between LDMC and both P_n and C_i in small trees, and between equivalent water thickness and both P_n and $_G$s in large trees. These findings underscore the importance of examining functional leaf traits to reveal species-specific responses to environmental changes. Such trait-based approaches can inform the design of resilient urban green spaces and contribute to a better understanding of how plant communities cope with environmental stressors in a changing climate.

RESULTS

Variation of leaf traits in large and small tree species

The study was conducted in Longzihu Park, Zhengzhou, China (**Figure 1**). This urban park features diverse tree species and represents a typical temperate city green space.

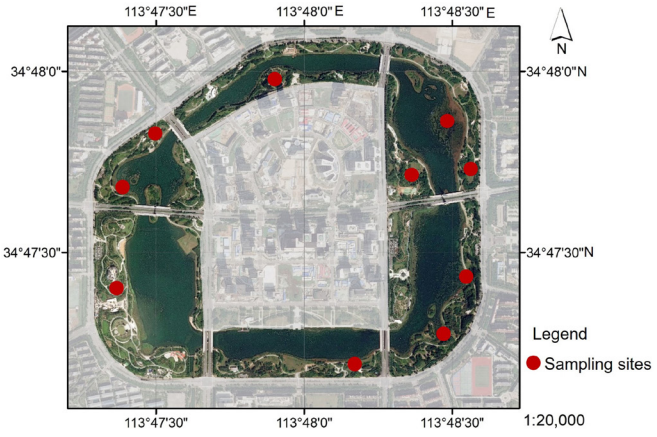

Figure 1: Map of study area (Longzi Lake Park, Zhengzhou, China) and sampling sites. The map presents the location of the study area and sampling sites. Basemap source: Tianditu (44). Map created by the authors using ArcGIS 10.6.

Type	Leaf trait (unit)	Min. (species)	Max. (species)	Median	Mean
Structural traits	LA (cm^2)	18.7 (*Magnolia denudata*)	150.2 (*Pterocarya tenoptera*)	99.5	83.7
	SLA ($cm^2 \cdot g^{-1}$)	95.6 (*Pterocarya stenoptera*)	288.1 (*Styphnolobium japonicum*)	144.0	166.1
	EWT ($g \cdot cm^{-2}$)	0.01 (*Syringa oblata*)	0.02 (*Ginkgo biloba*)	0.01	0.01
	LDMC ($g \cdot g^{-1}$)	0.27 (*Ginkgo biloba*)	0.50 (*Koelreuteria paniculata*)	0.36	0.37
Chemical traits	LCC ($mg \cdot g^{-1}$)	345.3 (*Pterocarya stenoptera*)	508.5 (*Syringa oblata*)	432.1	431.0
	LNC ($mg \cdot g^{-1}$)	11.9 (*Styphnolobium japonicum*)	31.8 (*Cercis chinensis*)	18.0	19.1
	LPC ($mg \cdot g^{-1}$)	1.3 (*Prunus serrulata*)	3.6 (*Magnolia denudata*)	2.4	2.5
	leaf N:P (N:P)	4.9 (*Magnolia denudata*)	14.6 (*Prunus serrulata*)	6.7	8.2
Photosynthetic traits	SPAD	31.0 (*Platanus orientalis*)	57.4 (*Koelreuteria paniculata*)	42.2	43.2
	P_n ($\mu mol \cdot m^{-2} \cdot s^{-1}$)	2.1 (*Koelreuteria paniculata*)	6.2 (*Prunus cerasifera*)	3.9	4.0
	C_i ($\mu mol \cdot m^{-2} \cdot s^{-1}$)	250.6 (*Pterocarya stenoptera*)	401.8 (*Prunus cerasifera*)	305.5	306.3
	G_s ($\mu mol \cdot m^{-2} \cdot s^{-1}$)	0.05 (*Styphnolobium japonicum*)	0.19 (*Cercis chinensis*)	0.10	0.10

Table 1: Statistical information on the variation of leaf traits across ten deciduous broadleaf tree species (n = 60). LA, leaf area; SLA, specific leaf area; EWT, equivalent water thickness; LDMC, leaf dry matter content; LCC, leaf carbon content; LNC, leaf nitrogen content; LPC, leaf phosphorus content; leaf N:P, leaf nitrogen-to-phosphorus ratio; SPAD, soil and plant analyzer development; P_n, net photosynthetic rate; C_i, intercellular CO_2 concentration; G_s, stomatal conductance.

Trees were categorized into large and small growth forms based on DBH and height. Leaf samples were analyzed for selected structural traits (e.g., SLA, LDMC), chemical traits (e.g., LNC, LPC), and physiological parameters (*P*n, *C*i, *G*s).

The maximum and minimum values across structural, chemical, and physiological traits highlighted the unique ecological strategies of different tree species (**Table 1**). In general, small trees had higher SLA and leaf N:P, while large trees had higher LA, equivalent water thickness and LPC (**Figure 2**). Photosynthetic traits also varied with size; small trees generally showed higher P_n, C_i, and G_s, while no significant difference was observed in relative chlorophyll content (SPAD) (**Figure 2**). For structural traits, *Styphnolobium japonicum*, classified as a small tree species, had the highest SLA (288.1 $cm^2 \cdot g^{-1}$), which represents leaf area per unit dry mass and reflects a trade-off between rapid growth and structural investment (15). In contrast, *Pterocarya stenoptera*, one of the large tree species, had the lowest SLA (95.6 $cm^2 \cdot g^{-1}$). Equivalent water thickness, which quantifies water content per unit leaf area and indicates water retention capacity, was highest in *Ginkgo biloba* (large tree, 0.02 $g \cdot cm^{-2}$) and lowest in *Syringa oblata* (small tree, 0.01 $g \cdot cm^{-2}$) (16). For chemical traits, *Cercis chinensis* (a small tree) exhibited the highest LNC (31.8 $mg \cdot g^{-1}$), while *Styphnolobium japonicum* (a large tree) had the lowest (11.9 $mg \cdot g^{-1}$). *Magnolia denudata* (a large tree) had the highest LPC (3.6 $mg \cdot g^{-1}$), whereas *Prunus serrulata* (a small tree) showed the lowest (1.3 $mg \cdot g^{-1}$). The leaf N:P ratio was highest in *Prunus serrulata* (14.6) and lowest in *Magnolia denudata* (4.9). Regarding photosynthetic traits, *Prunus cerasifera* (a small tree) demonstrated the highest P_n (6.2 $\mu mol \cdot m^{-2} \cdot s^{-1}$) and C_i (401.8 $\mu mol \cdot m^{-2} \cdot s^{-1}$), while *Koelreuteria paniculata* (a large tree) and *Pterocarya stenoptera* (a large tree) displayed the lowest P_n (2.1 $\mu mol \cdot m^{-2} \cdot s^{-1}$) and C_i (250.6 $\mu mol \cdot m^{-2} \cdot s^{-1}$), respectively.

Two-sample *t*-tests for each leaf trait showed varying patterns of differences between large and small tree species. For structural traits, large trees displayed higher LA ($p < 0.001$,

https://doi.org/10.59720/25-029

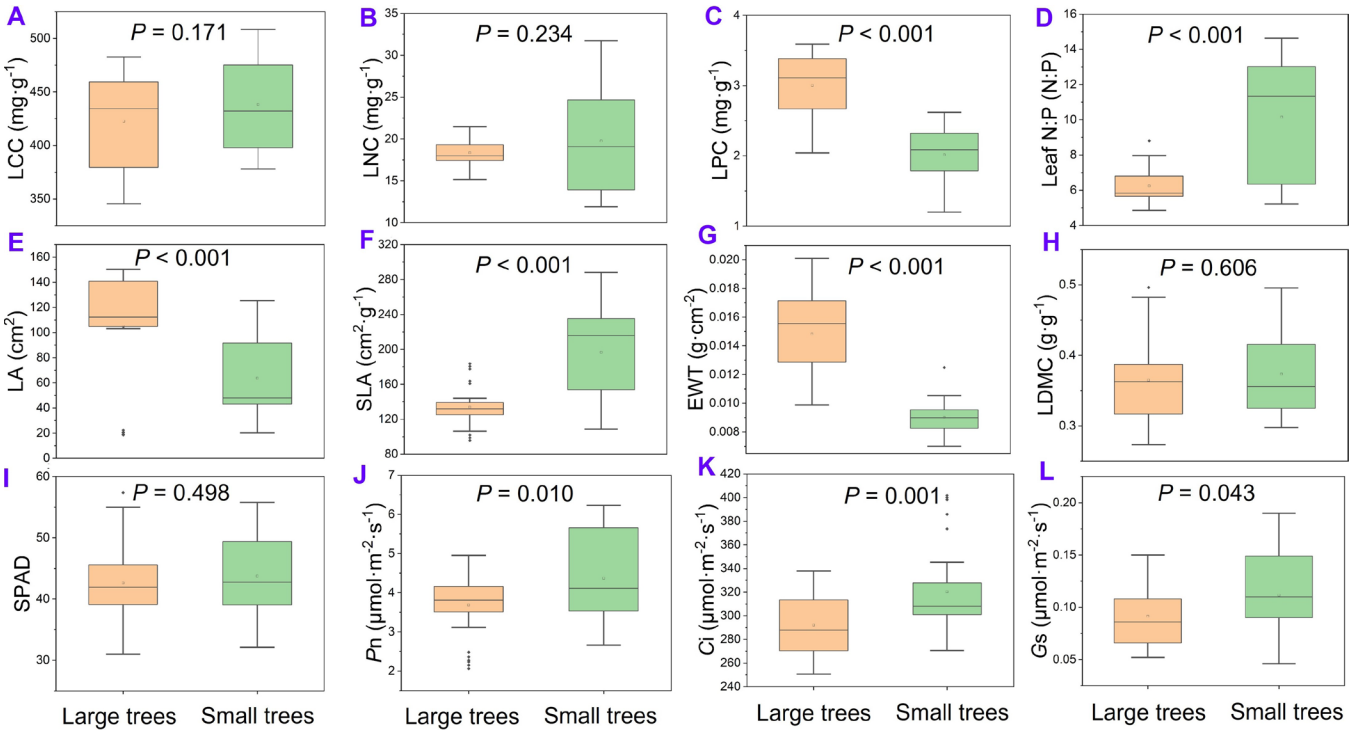

Figure 2: Comparison of leaf trait indicators between large and small deciduous tree species (n = 30). Different colors represent large and small trees. Distribution of **(A)** leaf carbon content (LCC), **(B)** leaf nitrogen content (LNC), **(C)** leaf phosphorus content (LPC), **(D)** leaf nitrogen-to-phosphorus ratio (leaf N:P), **(E)** leaf area (LA), **(F)** specific leaf area (SLA), **(G)** equivalent water thickness (EWT), **(H)** leaf dry matter content (LDMC), **(I)** soil and plant analyzer development (SPAD), **(J)** net photosynthetic rate (P_n), **(K)** intercellular CO_2 concentration (C_i), and **(L)** stomatal conductance (G_s) between large and small trees. P values above the bars were calculated using two-sample t-tests.

Figure 2E) and equivalent water thickness than small trees (p < 0.001, **Figure 2G**), reflecting their resource conservation strategies. In contrast, small trees had higher SLA, facilitating efficient light capture and photosynthesis (p < 0.001, **Figure 2F**). For chemical traits, LCC and LNC showed no differences between the two growth forms (LCC: p = 0.171, **Figure 2A**; LNC: p = 0.234, **Figure 2B**), suggesting conserved carbon storage and nitrogen investment across species. Large trees displayed higher LPC than small tress (p < 0.001, **Figure 2C**), suggesting superior phosphorus acquisition and storage. Conversely, the leaf N:P ratio was higher in small trees (p < 0.001, **Figure 2D**), highlighting their reliance on nitrogen-use efficiency in nutrient-limited environments. Photosynthetic traits varied notably between large and small tree species. Small tree species exhibited higher P_n, C_i, and G_s than large trees (P_n: p < 0.05, **Figure 2J**; C_i: p < 0.01, **Figure 2K**; G_s: p < 0.05, **Figure 2L**), suggesting a strategy of enhancing carbon assimilation through increased stomatal activity. However, SPAD values showed no significant differences between the two growth forms (p = 0.498, p > 0.05, **Figure 2I**), suggesting their similar chlorophyll content and sustained photosynthetic performance over time.

Relationships of leaf traits in large and small tree species

Pearson correlation analysis revealed distinct relationships among leaf traits. For large trees, LCC correlated positively with leaf N:P (r = 0.516, p < 0.01), SLA (r = 0.450, p < 0.05), and SPAD (r = 0.581, p < 0.001), but negatively with LPC (r = –0.591, p < 0.001) and LA (r = –0.427, p < 0.05) (**Figure 3**). LNC was positively related to LPC (r = 0.567, p < 0.001) and negatively to C_i (r = –0.571, p < 0.001) (**Figure 3**). LPC correlated positively with equivalent water thickness (r = 0.539, p < 0.01) and P_n (r = 0.704, p < 0.001), and negatively with leaf N:P (r = –0.892, p < 0.001), SLA (r = –0.431, p < 0.05), and LDMC (r = –0.624, p < 0.001) (**Figure 3**). Leaf N:P was positively associated with LDMC (r = 0.736, p < 0.001) and negatively with equivalent water thickness and P_n (both r = –0.695, p < 0.001) (**Figure 3**). LA correlated positively with LDMC (r = 0.609, p < 0.001) but negatively correlated with equivalent water thickness (r = –0.606, p < 0.001), P_n (r = –0.456, p < 0.05), and G_s (r = –0.724, p < 0.001) (**Figure 3**). Equivalent water thickness was negatively related to SLA (r = –0.604, p < 0.05) and LDMC (r = –0.555, p < 0.01) but positively to P_n (r = 0.378, p < 0.05) and G_s (r = 0.425, p < 0.05) (**Figure 3**). LDMC correlated positively with SPAD (r = 0.470, p < 0.01) and negatively correlated with P_n (r = –0.874, p < 0.001). G_s was positively correlated with SPAD (r = 0.485, p < 0.01) (**Figure 3**). Other leaf traits pairs were not significantly correlated (all p > 0.05) (**Figure 3**).

For small trees, LCC showed positive correlations with LNC (r = 0.517, p < 0.01), P_n (r = 0.738, p < 0.001), and G_s (r = 0.572, p < 0.001), and negative correlations with equivalent water thickness (r = –0.692, p < 0.001) and C_i (r = –0.457, p < 0.05) (**Figure 3**). LNC related positively to leaf N:P (r = 0.811, p < 0.001), SLA (r = 0.421, p < 0.05), SPAD (r = 0.698, p < 0.001), and G_s (r = 0.763, p < 0.001), and negatively to equivalent water thickness (r = –0.404, p < 0.05) and C_i (r = –0.654, p < 0.001) (**Figure 3**). LPC correlated positively with P_n (r = 0.408, p < 0.05) and negatively with leaf N:P (r = –0.521, p < 0.01) (**Figure 3**). Leaf N:P positively correlated with SLA (r = 0.364, p < 0.05), SPAD (r = 0.804, p < 0.001), and G_s (r = 0.587, p < 0.001), and negatively with C_i (r = –0.762, p <

https://doi.org/10.59720/25-029

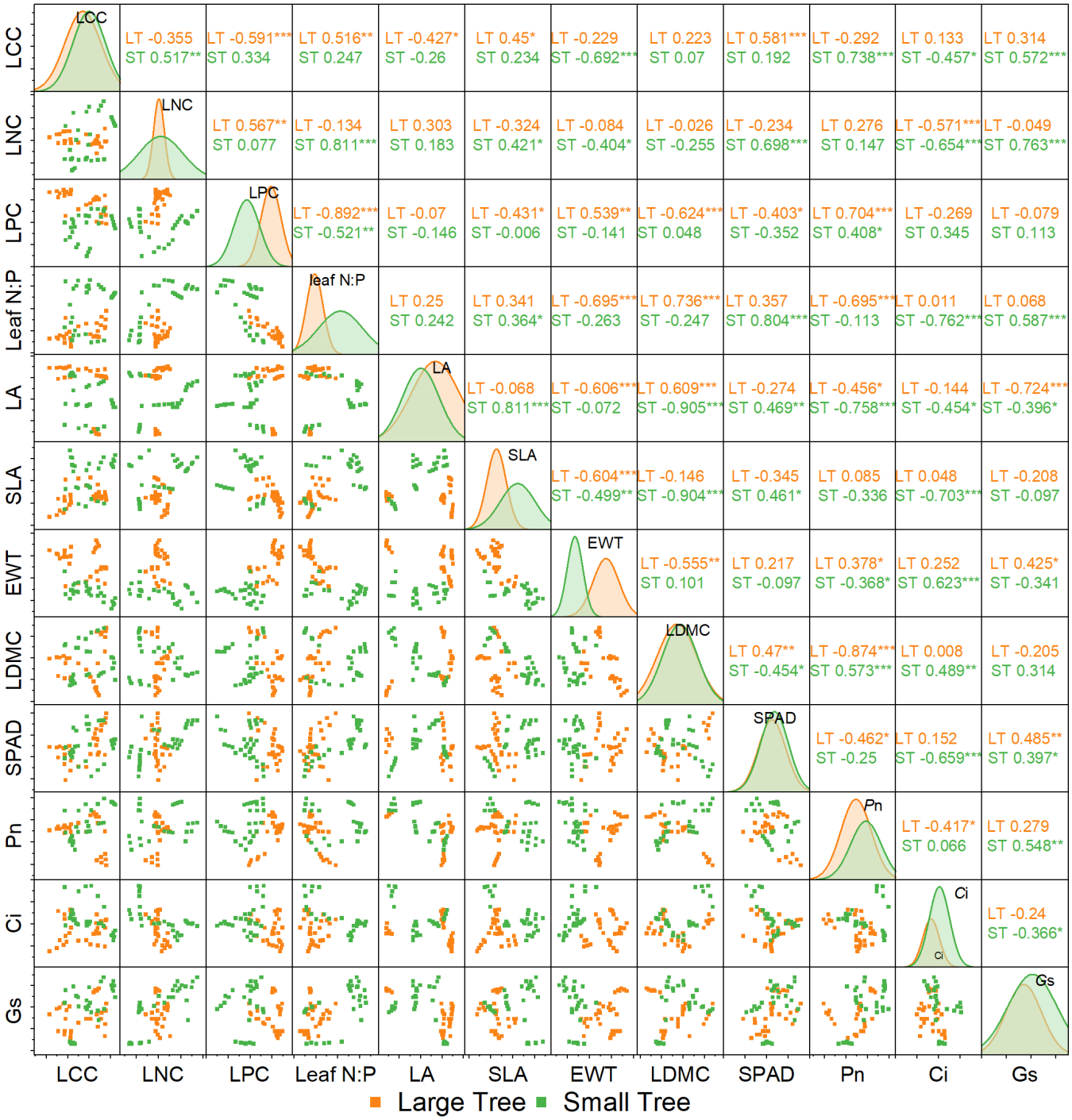

Figure 3: Correlation analysis of leaf traits in large and small tree species. In the upper-right boxes, Pearson correlation coefficients and their corresponding significance test results are presented for leaf trait pairs of large trees (LT, n = 30) and small trees (ST, n = 30), respectively. Significance levels are indicated by: p < 0.05 (*), p < 0.01 (**), and p < 0.001 (***). The diagonal boxes show the normal distribution fitting curves of leaf trait indicators for large trees (n = 30) and small trees (n = 30), while the bottom-left boxes display pairwise scatterplots of these traits for the two size classes.

0.001) (**Figure 3**). LA aligned positively with SLA (r = 0.811, p < 0.001) and SPAD (r = 0.469, p < 0.01), and negatively with LDMC (r = –0.905, p < 0.001), P_n (r = –0.758, p < 0.001), C_i (r = –0.454, p < 0.05), and G_s (r = –0.396, p < 0.05) (**Figure 3**). SLA was positively related to SPAD (r = 0.461, p < 0.05) and negatively to equivalent water thickness (r = –0.499, p < 0.01), LDMC (r = –0.904, p < 0.001), and C_i (r = –0.703, p < 0.001) (**Figure 3**). Equivalent water thickness co-varied positively with C_i (r = 0.623, p < 0.001) and negatively with P_n (r = –0.368, p < 0.05) (**Figure 3**). LDMC showed positive correlations with P_n (r = 0.573, p < 0.001) and C_i (r = 0.489, p < 0.01) and a negative correlation with SPAD (r = –0.454, p < 0.05) (**Figure 3**). SPAD was positively correlated with G_s (r = 0.397, p < 0.05) and negatively with C_i (r = –0.659, p <

https://doi.org/10.59720/25-029

0.001) (**Figure 3**). G_s positively correlated with P_n (r = 0.548, p < 0.01) and negatively with C_i (r = –0.366, p < 0.05) (**Figure 3**). Other leaf traits pairs were not significantly correlated (all p > 0.05) (**Figure 3**).

Regression analysis highlighted varying relationships of structural and chemical traits with photosynthetic traits. In small trees, LA was positively related to SPAD (*slope* = 0.122, p = 0.009; **Figure 4A**) and negatively related to P_n (*slope* = –0.344, p < 0.001; **Figure 4B**), C_i (*slope* =–0.086, p = 0.012; **Figure 4C**), and G_s (*slope* = –0.312, p = 0.030; **Figure 4D**). For large trees, LA was negatively related to P_n (*slope* = –0.157, p = 0.011; **Figure 4B**) and G_s (*slope* = –0.317, p < 0.001; **Figure 4D**) but showed no significant relationship with SPAD (p = 0.142; **Figure 4A**) or C_i (p = 0.448; **Figure 4C**). For small trees, SLA showed a positive relationship with SPAD (*slope* = 0.233, p < 0.05; **Figure 4E**) but a negative relationship with C_i (*slope* = –0.260, p < 0.001; **Figure 4G**), while showing no significant relationship with G_s (p = 0.610; **Figure 4H**). For large trees, SLA showed no significant relationships with any photosynthetic traits: SPAD (p = 0.062; **Figure 4E**), P_n (p = 0.654; **Figure 4F**), C_i (p = 0.801; **Figure 4G**), or G_s (p = 0.271; **Figure 4H**). Equivalent water thickness in large tree species showed positive relationships with P_n (*slope* = 0.482, p < 0.05; **Figure 4J**) and G_s (*slope* = 0.689, p < 0.05; **Figure 4L**) but was not significantly related to SPAD (p = 0.249; **Figure 4I**) or C_i (p = 0.179; **Figure 4K**). In small tree species, equivalent water thickness showed a positive relationship with C_i (*slope* = 0.563, p < 0.001; **Figure 4K**) and a negative relationship with G_s (*slope* = –1.261, p < 0.05; **Figure 4L**), while showing no significant relationships with SPAD (p = 0.612; **Figure 4I**)

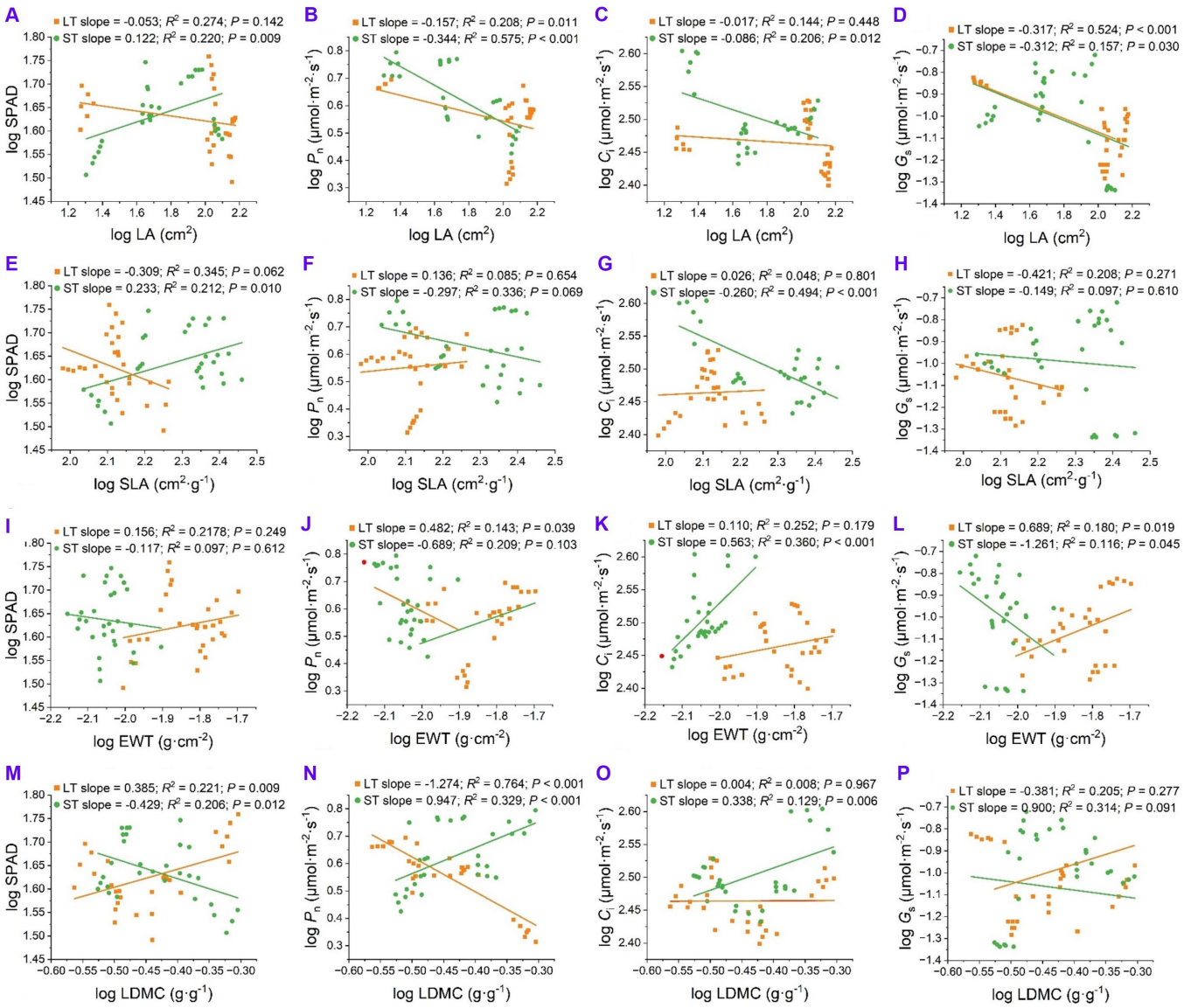

Figure 4: Regression analyses of leaf structural traits with physiological traits in large and small tree species. Large trees (LT) and small trees (ST) are represented by different colors. Relationships of **(A)** LA with SPAD, **(B)** LA with P_n, **(C)** LA with C_i, **(D)** LA with G_s, **(E)** SLA with SPAD, **(F)** SLA with P_n, **(G)** SLA with C_i, **(H)** SLA with G_s, **(I)** EWT with SPAD, **(J)** EWT with P_n, **(K)** EWT with C_i, **(L)** EWT with G_s, **(M)** LDMC with SPAD, **(N)** LDMC with P_n, **(O)** LDMC with C_i and **(P)** LDMC with G_s. The regression function was expressed as $y = bx^a$, transformed into log y = log b + a·log x, where x and y represent two trait parameters, log b denotes the intercept, and a indicates the slope. Linear regression was used to obtain slope, p-value, and R^2 values.

https://doi.org/10.59720/25-029

or P_n (p = 0.103; **Figure 4J**). LDMC showed relationships with P_n in large (*slope* = –1.274, p < 0.001) and small trees (*slope* = 0.947, p < 0.001; **Figure 4N**), and with SPAD in large (*slope* = 0.385, p < 0.01) and small trees (*slope* = -0.429, p < 0.05; **Figure 4M**). However, LDMC did not show significant relationships with G_s in either large (p = 0.277) or small trees (p = 0.091; **Figure 4P**).

Chemical traits had pronounced relationships with photosynthetic performance. For small trees, LCC was positively related to P_n (*slope* = 1.995, p < 0.001; **Figure 5B**) and G_s (*slope* = 2.687, p < 0.001; **Figure 5D**), negatively related to C_i (slope = –0.517, p = 0.011; **Figure 5C**), and had no significant relationships with SPAD (p = 0.309; **Figure 5A**). LNC in small trees was positively related to SPAD (*slope* = 0.327, p < 0.001; **Figure 5E**) and G_s (*slope* = 1.089, p < 0.001; **Figure 5H**), negatively related to C_i (*slope* = –0.224, p < 0.001; **Figure 5G**), but had no significant relationships with P_n (p = 0.437; **Figure 5F**). For small trees, LPC had a negative relationship with SPAD (*slope* = –0.240, p = 0.048; **Figure 5I**), positive relationship with P_n (*slope* = 0.488, p = 0.025; **Figure 5J**) and C_i (*slope* = 0.173, p = 0.046; **Figure 5K**), and no significant relationship with G_s (p = 0.552; **Figure 5L**). Leaf N:P ratios positively influenced SPAD (*slope* = 0.323, p < 0.001; **Figure 5M**) and G_s (*slope* = 0.717, p < 0.001; **Figure 5P**), negatively related to C_i (*slope* = –0.224, p < 0.001; **Figure 5O**), and had no significant relationship with P_n (p = 0.551; **Figure 5N**). In contrast, for large tree species, LCC positively related to SPAD (*slope* = 0.796, p < 0.001; **Figure 5A**) and had no significant relationship with P_n (p = 0.118; **Figure 5B**), C_i (p = 0.483; **Figure 5C**), and G_s (p = 0.722; **Figure 5D**). LNC showed a negative relationship with C_i (*slope* = –0.625, p < 0.001; **Figure 5G**) but had no significant relationship with

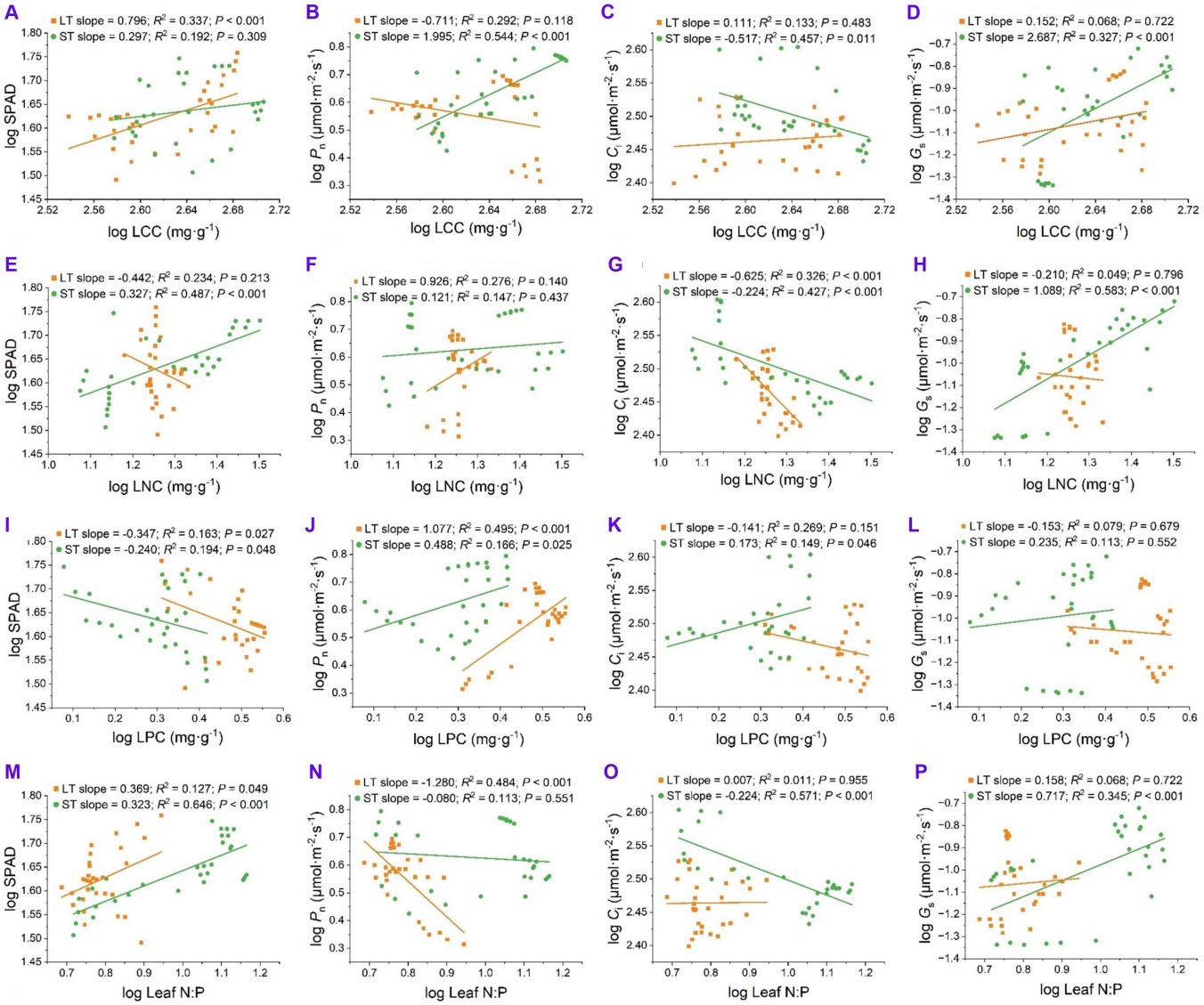

Figure 5: Regression analyses of leaf chemical traits with physiological traits in large and small tree species. Large trees (LT) and small trees (ST) are represented by different colors. Relationships of **(A)** LCC with SPAD, **(B)** LCC with P_n, **(C)** LCC with C_i, **(D)** LCC with G_s, **(E)** LNC with SPAD, **(F)** LNC with P_n, **(G)** LNC with C_i, **(H)** LNC with G_s, **(I)** LPC with SPAD, **(J)** LPC with P_n, **(K)** LPC with C_i, **(L)** LPC with G_s, **(M)** leaf N:P with SPAD, **(N)** leaf N:P with P_n, **(O)** leaf N:P with C_i, and **(P)** leaf N:P with G_s. The regression function was expressed as $y = bx^a$, transformed into log y = log b + alog x, where x and y represent two trait parameters, log b denotes the intercept, and a indicates the slope. Linear regression was used to obtain slope, p-value, and R^2 values.

https://doi.org/10.59720/25-029

SPAD (p = 0.213; **Figure 5E**), P_n (p = 0.140; **Figure 5F**), or G_s (p = 0.796; **Figure 5H**). LPC negatively related to SPAD (*slope* = –0.347, p = 0.027; **Figure 5I**), positively related to P_n (*slope* = 1.077, p < 0.001; **Figure 5J**), and had no significant relationship with C_i (p = 0.151; **Figure 5K**), or G_s (p = 0.679; **Figure 5L**). Leaf N:P ratios positively related to SPAD (*slope* = 0.369, p = 0.049; **Figure 5M**), negatively related to P_n (*slope* = –1.280, p < 0.001; **Figure 5N**), and had no significant relationship with C_i (p = 0.955; **Figure 5O**). or G_s (p = 0.722; **Figure 5P**).

Trade-off patterns of leaf traits in large and small tree species

Principal component analysis (PCA) of structural, chemical, and photosynthetic traits revealed key trade-offs in leaf ecological functions and drivers of variability (**Figure 6**). For leaf structural traits, the first two principal components (PC1 and PC2) explained 74.1% of the variation (**Figure 6A**). PC1 primarily represented leaf size and thickness, as indicated by strong loadings of leaf area and equivalent water thickness, while PC2 was associated with tissue density, mainly reflecting variations in LDMC and SLA. Specifically, along PC1, equivalent water thickness and LDMC were positively correlated (**Figure 6A**), indicating a co-variation that may be related to leaf structural properties. Along PC2, equivalent water thickness and SLA were negatively correlated, indicating that these traits varied in opposite direction in the principal component space. Compared with large tree species, small tree species were distributed toward the PCA axes associated with SLA and LDMC, whereas large tree species were distributed closer to the axes associated with equivalent water thickness and LA (**Figure 6A**).

For leaf chemical traits, PC1 and PC2 explained 80.7% of the variation collectively (**Figure 6B**). The leaf N:P ratio and LCC were the dominant contributors along PC1, while LPC and LNC were the main contributors to PC2, together explaining differences between small and large tree species. For photosynthetic physiological traits, PC1 and PC2 accounted for 40.5% and 33.8% of the variation, respectively (**Figure 6C**). Along PC1, SPAD and G_s had the largest positive loadings, while along PC2, C_i and P_n had loadings of opposite sign (C_i negative, P_n positive) (**Figure 6C**). When integrating all traits, PC1 and PC2 highlighted distinct trade-offs between large and small tree species. PC1 was predominantly influenced by all chemical traits and structural traits (SLA, equivalent water thickness), while PC2 was primarily associated with physiological traits (P_n, C_i, G_s) and LDMC (**Figure 6D**).

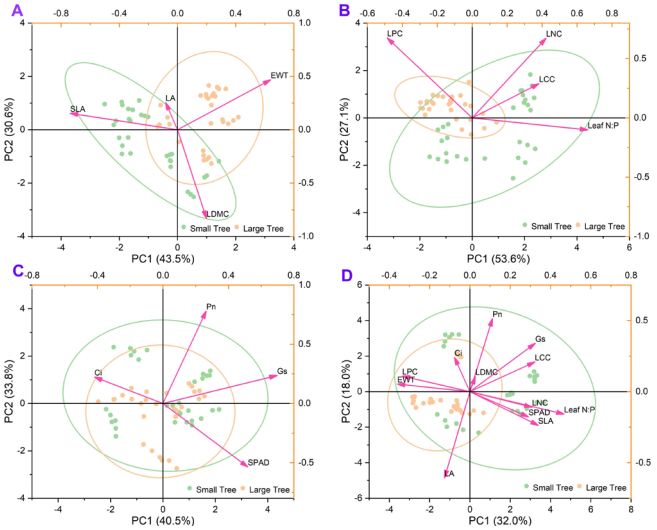

Figure 6: Principal component analysis (PCA) of leaf traits across different growth forms. Panels show ordination based on **(A)** leaf structural traits, **(B)** chemical traits, **(C)** photosynthetic physiological traits, and **(D)** all traits. Pink arrows represent the principal component loadings, indicating the contribution of each leaf trait to the principal components. The points represent individual tree species projected onto the principal component space. Samples are plotted in the two-dimensional space defined by the first two principal components (PC1 and PC2). The percentages shown on the axes indicate the proportion of the total variance in the dataset explained by each principal component. The circles represent 95% confidence ellipses for each group, calculated from the covariance of the samples within each group. The orange axes represent the variable loadings, showing how each trait contributes to PC1 and PC2.

DISCUSSION

In this study, we hypothesized that large and small deciduous broadleaf trees differ in the variation, relationships, and trade-offs of leaf traits. To test this, we classified tree species by size (large and small) and examined their leaf traits. Distinct leaf trait strategies were observed among species. In general, small trees tended to exhibit higher SLA, LNC, and leaf N:P, but lower LA, equivalent water thickness, and LPC (**Table 1, Figure 2**). Some species, however, deviated from this general trend. For example, the small tree species *Styphnolobium japonicum* exhibited the lowest LNC across all measured trees, likely reflecting its adaptation to nutrient-poor soils and a conservative nutrient-use strategy that emphasizes leaf longevity rather than rapid growth (17). In contrast, the large tree species *Magnolia denudata* showed the smallest LA across all measured trees, a trait consistent with shade-tolerant strategies and structural adaptations to low-light conditions, where smaller leaves help reduce water loss while maintaining efficient light capture under the canopy (18).

Large tree species demonstrated significantly greater LA and equivalent water thickness compared to small tree species (**Figure 2**). This finding suggests that large trees optimize photosynthetic efficiency through larger leaves, while small tree species reduce leaf area to minimize water loss under high light intensity (19). These results are consistent with prior studies on leaf trait adaptations (5,12, 20). Additionally, small tree species exhibited higher SLA and LNC, reflecting a strategy favoring rapid growth and resource acquisition (**Figure 2**). Previous studies did not report consistent LNC differences between smaller and larger trees (1, 13, 14). This may reflect species- or site-specific allocation strategies in response to light and nutrient availability. These resource-acquisitive traits are characteristic of plants adapted to fluctuating resource environments (2, 3, 21). Small trees have been shown to exhibit higher P_n, C_i, and G_s compared to large trees, highlighting adaptive strategies to maximize carbon gain under fluctuating light and resource-abundant environments (22). These observations underscore the ecological divergence between large and small trees, with growth forms driving functional trait variation and contributing to ecosystem stability (23).

https://doi.org/10.59720/25-029

The relationships between leaf traits varied between large and small deciduous tree species. For large trees, equivalent water thickness showed significant positive relationships with P_n and G_s (**Figure 4**). In contrast, small tree species exhibited significant positive correlations between LDMC and P_n, as well as between LDMC and C_i (**Figure 3**). These patterns suggest that small trees optimize photosynthesis by balancing structural investments and physiological performance, consistent with the trade-off framework (24). In small trees, both LPC and LCC were positively correlated with P_n, whereas in large trees, only LPC exhibited a significant positive correlation with P_n (**Figure 3**). This difference may reflect the critical role of phosphorus in photosynthesis, as it is essential for the synthesis of adenosine triphosphate, energy production, and the formation of genetic material (25). In contrast, the influence of LCC on P_n appears more pronounced in small trees, possibly because small trees allocate more carbon resources to leaf construction than large trees to maximize photosynthetic capacity (26).

SLA was positively correlated with LCC, LNC, and leaf N:P in small trees, where higher SLA indicates thinner leaves and larger leaf areas, facilitating increased photosynthetic efficiency and resource capture (**Figure 3**) (27). These morphological traits enable small tree species to optimize resource acquisition in competitive environments (28).

The trade-offs between different growth forms underscore the diversity of strategies for resource acquisition and environmental adaptation. Our results suggest a distinct trade-off between SLA and P_n in small trees species, which supports a preference for rapid resource acquisition at the expense of structural stability (29). These findings are consistent with the leaf economics spectrum theory, which describes a continuum of plant strategies ranging from conservative, resource-conserving traits to acquisitive, rapid-growth traits (12). Small trees exhibited higher LCC, which was positively correlated with photosynthetic traits such as P_n and G_s (**Figure 2A, 3**). These traits indicate an emphasis on nutrient allocation for rapid metabolic activity and photosynthesis, favoring short-term resource acquisition (24, 30). In contrast, large tree species showed higher LPC, supporting enzymatic and metabolic processes associated with long-term resource conservation and utilization efficiency (31).

PCA of structural traits suggested that large and small trees may adopt divergent functional strategies. Large trees tend to invest in traits related to stability and water retention, which could reflect a resource-conservation strategy that helps them withstand environmental stresses such as drought or mechanical damage (14, 21). In contrast, small trees appear to emphasize higher SLA, which may support rapid carbon assimilation and growth to compete for light in dense stands, reflecting an adaptive strategy for optimizing resource use efficiency and maintaining structural integrity (5, 14). These patterns highlight a possible trade-off between fast growth and conserving resources, showing how a tree's size may affect how it distributes resources to survive and thrive under changing environmental conditions (3, 11).

Several limitations should be acknowledged. First, only 12 key traits were analyzed, excluding factors such as leaf mechanical strength and hydraulic properties, which could offer a fuller view of plant strategies (32). Second, the study relied on data from a single urban area and a one-time survey, limiting generalizability and causal inference; multi-site, longitudinal studies are needed to reveal the mechanisms driving trait variability (33).

The study highlights the variability and adaptive strategies of leaf functional traits across tree growth forms. Previous research has shown that trees with high LDMC and low SLA are more resilient to urban stressors like heat and pollution (34). Moreover, previous studies suggest that species with higher photosynthetic capacity and water-use efficiency may better tolerate fluctuating water availability (35). Although water availability dynamics were not explicitly evaluated here, the trait patterns observed are consistent with previous findings indicating that large trees with resource-conserving traits tend to thrive in stable urban settings, while smaller trees may support rapid canopy development in disturbed areas, potentially contributing to urban heat island mitigation (35). Understanding these functional traits can guide species selection in urban planning, enhancing green space resilience. Fast-growing species may be suitable for rapid vegetation establishment, and diverse mixes can maximize ecosystem services, including temperature regulation, carbon sequestration, and air purification (36).

MATERIALS AND METHODS

Study area overview

The study was conducted in Zhengzhou, Henan Province, China (34°16′–34°58′N, 112°42′–114°14′E). The region has a warm temperate continental monsoon climate, with an average annual sunshine duration of 1904.7 hours and an average temperature of 15.4°C. The annual average frost-free period is 212.6 days, with an annual precipitation of approximately 632.4 mm, primarily concentrated from June to August (37).

Sample collection

Sample collection was carried out between June and July 2024 in Longzi Lake Park, Zhengzhou, China (**Figure 1**). Based on a comprehensive field survey, ten deciduous broadleaf tree species were selected to represent two distinct growth forms: large trees, defined as woody plants with DBH ≥ 5 cm and height (H) ≥ 5 m, and small trees, defined as woody plants with DBH < 5 cm and H < 5 m (38). Large tree species included *Magnolia denudata*, *Koelreuteria paniculata*, *Platanus orientalis*, *Ginkgo biloba*, and *Pterocarya stenoptera*, while small tree species comprised of *Syringa oblata*, *Cercis chinensis*, *Styphnolobium japonicum*, *Prunus cerasifera*, and *Prunus serrulata var. lannesiana*.

For each tree species, six healthy, mature individuals exhibiting uniform growth were selected. Sampling involved selecting five branches from four cardinal directions (east, west, south, and north) on each individual tree. For each branch, 10 healthy, fully expanded, pest-free leaves were collected, resulting in 50 leaves per tree. Samples were immediately placed in sealed, moistened bags and transported to the laboratory under cool conditions (4–8°C) to minimize physiological changes before analysis.

Measurement of leaf chemical traits

LCC, LNC, LPC and leaf N:P ratios were measured using ground leaf samples. LCC was measured via external heating with potassium dichromate ($K_2Cr_2O_7$) (41). Briefly, 0.200 g of ground leaf sample was digested with 10 mL of 0.8 mol·L^{-1} $K_2Cr_2O_7$ and 10 mL of concentrated sulfuric acid

https://doi.org/10.59720/25-029

(98% H2SO4) in a digestion tube. The mixture was heated at 170°C for 30 minutes to oxidize organic carbon. After cooling, the digest was diluted to 100 mL with distilled water, and the excess dichromate was titrated with 0.2 mol·L^{-1} ferrous sulfate ($FeSO_4$) using ferroin as an indicator (39). LNC was determined using the Kjeldahl digestion method (40). About 0.300 g of dried leaf sample was digested with 10 mL of 98% H_2SO_4 and a catalyst mixture [potassium sulfate (K_2SO_4) and copper sulfate ($CuSO_4$), 10:1] at 420°C for 1 hour. After cooling, the digest was neutralized with sodium hydroxide (NaOH), distilled to release ammonia, which was trapped in 2% boric acid (H3BO3), and titrated with 0.01 mol·L^{-1} hydrochloric acid (HCl) (40). LPC was measured using the molybdenum-antimony colorimetric method (42). Samples were digested with 98% H_2SO_4, followed by the gradual addition of hydrogen peroxide (30% H_2O_2) until the solution became clear. The digested samples were then mixed with a colorimetric reagent containing ammonium molybdate [$(NH_4)_6Mo_7O_{24}\cdot4H_2O$, 35.6 g·L^{-1}] and potassium antimony tartrate ($C_4H_4KO_7Sb$, 3 g·L$^{-1)}$ in 1 mol·L^{-1} H_2SO_4, followed by reduction with ascorbic acid ($C_6H_8O_6$, 18 g·L^{-1}). The resulting blue complex was measured spectrophotometrically at 880 nm using a UV–Vis spectrophotometer (Shimadzu UV-2600, Shimadzu Corporation, Japan), and LPC was calculated from a standard calibration curve prepared with known phosphate standards (40). The leaf N:P ratio was calculated as: Leaf N:P = LNC (mg·g^{-1})/LPC (mg·g^{-1}).

Measurement of leaf structural traits

Four leaf structural traits (LA, SLA, equivalent water thickness, and LDMC) were measured following standardized protocols for plant functional traits (16). Specifically, fresh weight was measured after removing petioles using an electronic balance (accuracy: 0.1 mg). For leaf area measurement, leaves were flattened and scanned using a Lide 400 scanner (Canon, Japan), and the scanned images were analyzed using ImageJ (version 2) software (41). The scanned leaves were then oven-dried at 75°C until no more change in mass was observed. SLA, equivalent water thickness, and LDMC were determined using the following equations:

$$\text{SLA} = \text{LA (cm}^2\text{)} / \text{leaf dry mass (g)}$$

$$\text{Equivalent water thickness} = (\text{leaf fresh mass (g)} - \text{leaf dry mass (g)}) / \text{LA (cm}^2\text{)}$$

$$\text{LDMC} = \text{leaf dry mass (g)} / \text{leaf saturated fresh mass (g)}$$

Measurement of photosynthetic traits

Photosynthetic traits (P_n, C_i, and G_s) were measured under clear, windless conditions using an LCPro-SD portable photosynthesis system (ADC BioScientific, UK) according to the manufacturer›s instructions. Measurements were taken between 8:00 and 18:00 at 2-hour intervals, using three sun-exposed leaves per tree at each time point; different leaves were measured each time, and the mean value was used. For each species, five sunlit, fully expanded, and healthy leaves were selected from a representative tree. Measurements were repeated three times per leaf, and the average value was recorded. Additionally, SPAD was measured using a SPAD-502 plus chlorophyll meter (Konica Minolta, Japan), which provides a unitless index indicating relative chlorophyll concentration based on leaf greenness. For each leaf, three SPAD readings were taken at different positions avoiding the midrib, and the average value was calculated. Measurements were conducted between 09:00 a.m. and 11:00 a.m., with each measurement performed on a different leaf.

Type	Leaf trait (unit)	Shapiro–Wilk test				Levene's test	
		Large trees		Small trees			
		W	*P*	*W*	*P*	*F*	*P*
Structural traits	LA (cm^2)	0.764	*< 0.001*	0.886	0.004	1.777	0.127
	SLA (cm^2·g^{-1})	0.927	0.042	0.920	0.028	0.173	*< 0.001*
	EWT (g·cm^{-2})	0.958	0.278	0.957	0.262	6.510	*< 0.001*
	LDMC (g·g^{-1})	0.907	0.012	0.914	0.019	1.229	0.582
Chemical traits	LCC (mg·g^{-1})	0.892	0.005	0.913	0.018	1.801	0.836
	LNC (mg·g^{-1})	0.942	0.101	0.899	0.008	0.052	*< 0.001*
	LPC (mg·g^{-1})	0.898	0.007	0.942	0.102	1.363	0.409
	leaf N:P	0.900	0.008	0.867	0.001	0.077	*< 0.001*
Photosynthetic traits	SPAD	0.967	0.459	0.958	0.267	0.941	0.871
	P_n(μmol·m^{-2}·s^{-1})	0.909	0.014	0.903	0.010	0.571	*< 0.001*
	C_i(μmol·m^{-2}·s^{-1})	0.950	0.173	0.853	0.001	1.988	0.069
	G_s(μmol·m^{-2}·s^{-1})	0.896	0.007	0.941	0.097	0.517	0.081

Table 2: Normality and homoscedasticity tests for trait datasets (n = 30). Normality was assessed with the Shapiro–Wilk test, reporting the statistic W and p. Homogeneity of variances was assessed with Levene's test, reporting the statistic F and p for the comparison between large and small trees. For the Shapiro–Wilk test, p ≥ 0.05 indicates the leaf trait is normal within small trees or large trees; for the Levene's test, p ≥ 0.05 indicates equal variances between small trees and large trees.

Data analysis

The normality of residual distributions and homoscedasticity of variances were examined for all datasets prior to statistical analyses (**Table 2**). Non-normal data were log-transformed before further tests. Differences between groups for each leaf trait were tested using two-sample *t*-tests (42). Pearson correlation analysis (two-tailed) was used to examine pairwise relationships among traits, using *t*-distribution with (*n*-2) degrees of freedom. Linear regression analyses, following logarithmic transformations of the data, were conducted to explore functional trait dependencies, with model evaluation based on the estimated slope, *p*-value, and coefficient of determination (R^2) (43).

Prior to PCA, all variables were standardized to a mean of 0 and a standard deviation of 1 using *Z*-score transformation (subtracting the mean and dividing by the standard deviation). We conducted four separate PCAs: leaf structural traits, chemical traits, photosynthetic physiological traits, and all traits combined. For each PCA, the eigenvalues and the proportion of variance explained were used to determine the number of principal components to retain, following the Kaiser criterion (eigenvalue > 1). The loadings of the retained components were examined to interpret the relationships among variables. For visualization, the first two principal components (PC1 and PC2) were retained in each PCA, representing the main axes of trait variation across species. All statistical analyses and figure generation were performed using OriginPro 2024 (OriginLab Corporation).

ACKNOWLEDGMENTS

We would like to express our gratitude to Henan Agricultural University for providing the necessary equipment and facilities for laboratory testing. We extend our thanks to Dr. Zhou Mengli for her invaluable guidance and expertise in data analysis.

Received: January 30, 2025
Accepted: April 15, 2025
Published: April 15, 2026

https://doi.org/10.59720/25-029

REFERENCES

1. Rosas, T., *et al*. „Adjustments and Coordination of Hydraulic, Leaf and Stem Traits along a Water Availability Gradient.“ *New Phytologist*, vol. 223, 2019, pp. 632–646. https://doi.org/10.1111/nph.15684
2. Liu, H., *et al*. „Can Evolutionary History Predict Plant Plastic Responses to Climate Change?“ *New Phytologist*, vol. 235, 2022, pp. 1260–1271. https://doi.org/10.1111/nph.18194
3. Huxley, J.D., *et al*. „Plant Functional Traits Are Dynamic Predictors of Ecosystem Functioning in Variable Environments.“ *Journal of Ecology*, vol. 111, 2023, pp. 2597–2613. https://doi.org/10.1111/1365-2745.14197.
4. Thakur, D., *et al*. „Differential Effect of Climate of Origin and Cultivation Climate on Structural and Biochemical Plant Traits.“ *Functional Ecology*, vol. 37, 2023, pp. 1436–1448. https://doi.org/10.1111/1365-2435.14291.
5. Wright, I. and M. Westoby. „Understanding Seedling Growth Relationships Through Specific Leaf Area and Leaf Nitrogen Concentration: Generalisations Across Growth Forms and Growth Irradiance.“ *Oecologia*, vol. 127, 2001, pp. 21–29. https://doi.org/10.1007/s004420000554.
6. Ordoñez, J.C., *et al*. „ A Global Study of Relationships Between Leaf Traits, Climate, and Soil Measures of Nutrient Fertility.“ *Global Ecology and Biogeography*, vol. 18, no. 1-2, 2009, pp.137-149. https://doi.org/10.1111/j.1466-8238.2008.00441.x
7. Piao, S., *et al*. „Net Carbon Dioxide Losses of Northern Ecosystems in Response to Autumn Warming.“ *Nature*, vol. 451, 2008, pp. 49–52. https://doi.org/10.1038/nature06444
8. Münzbergová, Z., *et al*. „Genetic Differentiation and Plasticity Interact along Temperature and Precipitation Gradients to Determine Plant Performance under Climate Change.“ *Journal of Ecology*, vol. 105, 2017, pp. 1358–1373. https://doi.org/10.1111/1365-2745.12762
9. Liang, X., *et al*. „Stomatal Responses of Terrestrial Plants to Global Change.“ *Nature Communications*, vol. 14, 2023, p. e2188. https://doi.org/10.1038/s41467-023-37934-7
10. Pérez-Ramos, I.M., *et al*. “Functional Traits and Phenotypic Plasticity Modulate Species Coexistence Across Contrasting Climatic Conditions.” *Nature Communications*, vol. 10, 2019, p. e2555. https://doi.org/10.1038/s41467-019-10453-0
11. Rowe, N. and T. Speck. “Plant Growth Forms: An Ecological and Evolutionary Perspective.” *New Phytologist*, vol. 166, 2005, pp. 61–72. https://doi.org/10.1111/j.1469-8137.2004.01309.x
12. Cui, E.Q., *et al*. “Robust Leaf Trait Relationships Across Species under Global Environmental Changes.” *Nature Communications*, vol. 11, no 1, 2020, p. e2999. https://doi.org/10.1038/s41467-020-16839-9
13. He, D. and E.R. Yan. “Size-Dependent Variations in Individual Traits and Trait Scaling Relationships Within a Shade-Tolerant Evergreen Tree Species.” *American Journal of Botany*, vol. 105, no. 7, 2018, pp. 1165–1174. https://doi.org/10.1002/ajb2.1132
14. Fan, H. K., *et al*. “ Leaf Trait Variation and Trade-Offs Among Growth Types of Broadleaf Plants in Xiao Hinggan Mountains.” *Chinese Journal Plant Ecology*, vol. 48, no. 3, 2024, pp. 364–376. https://doi.org/10.17521/cjpe.2023.0137
15. Niklas, K.J., *et al*. „Leaf Functional Traits: Ecological and Evolutionary Implications.“ *Frontiers in Plant Science*, vol. 14, 2023, p. e1169558. https://doi.org/10.3389/fpls.2023.1169558
16. Pérez-Harguindeguy, N., *et al*. *“Corrigendum to*: New Handbook for Standardised Measurement of Plant Functional Traits Worldwide.” *Australian Journal of Botany*, vol. 64, 2016, pp. 715–716. https://doi.org/10.1071/BT12225_CO
17. Su, Y. H., *et al*. “ Leaf Morphological and Nutrient Traits of Common Woody Plants Change Along the Urban–Rural Gradient in Beijing, China.” *Frontiers in Plant Science*, vol. 12, 2021, p. e682274. https://doi.org/10.3389/fpls.2021.682274
18. Mezui, E.N., et al. „ Light Tolerance-Related Tree Growth Strategies and Their Impacts on Key Functional Tree Traits: A Review.“ *BioResources*, vol. 19, no. 4, 2024, pp. 9946–9963. https://doi.org/10.15376/biores.19.4.NkeneMezui
19. Poorter, H., *et al*. „ Causes and Consequences of Variation in Leaf Mass per Area (LMA): A Meta-Analysis.“ *New Phytologist*, vol. 182, no. 3, 2009, pp. 565–588. https://doi.org/10.1111/j.1469-8137.2009.02830.x
20. Zheng, S.X. and Z.P. Shangguan. „Photosynthetic Characteristics and Their Relationships with Leaf Nitrogen Content and Leaf Mass per Area in Different Plant Functional Types.“ *Acta Ecologica Sinica*, vol. 27, 2007, pp. 171–181. https://www.ecologica.cn/stxb/article/abstract/1000-0933200701-0171-11(in Chinese)
21. Kühn, N., *et al*. “Globally Important Plant Functional Traits for Coping with Climate Change.” *Frontiers of Biogeography*, vol. 13, no. 4, 2021, p. e53774. https://doi.org/10.21425/F5FBG53774
22. Giles, A.L., *et al*. “ Small Understory Trees Have Greater Capacity Than Canopy Trees to Adjust Hydraulic Traits Following Prolonged Experimental Drought in a Tropical Forest.” *Tree physiology*, vol. 42, no. 3, 2022, pp. 537–556. https://doi.org/10.1093/treephys/tpab121
23. Hasper, T.B., *et al*. “Stomatal CO2 Responsiveness and Photosynthetic Capacity of Tropical Woody Species in Relation to Taxonomy and Functional Traits.” *Oecologia*, vol. 184, 2017, pp. 43–57. https://doi.org/10.1007/s00442-017-3829-0
24. He, P., *et al*. “Leaf Mechanical Strength and Photosynthetic Capacity Vary Independently Across 57 Subtropical Forest Species with Contrasting Light Requirements.” *New Phytologist*, vol. 223, 2019, pp. 607–618. https://doi.org/10.1111/nph.15803
25. Wright, I.J., *et al*. “The Worldwide Leaf Economics Spectrum.” *Nature*, vol. 428, 2004, pp. 821–827. https://doi.org/10.1038/nature02403
26. Lambers, H., *et al*. “Plant Nutrient-Acquisition Strategies Change with Soil Age.” *Trends in Ecology & Evolution*, vol. 23, 2008, pp. 95–103. https://doi.org/10.1016/j.tree.2007.10.008
27. Reich, P.B. “The World-Wide ‘Fast–Slow’ Plant Economics Spectrum: A Traits Manifesto.” *Journal of Ecology*, vol. 102, 2014, pp. 275–301. https://doi.org/10.1111/1365-2745.12211
28. Grime, J.P. *Plant Strategies, Vegetation Processes, and Ecosystem Properties*. John Wiley & Sons, 2006
29. Peng, Z.D., *et al*. „How Do Allometric Growth Patterns

https://doi.org/10.59720/25-029

and Resource Strategies of An Invasive Hydrophyte Differ Between Island and Mainland Habitats?“ *Global Ecology and Conservation*, 2024, p. e03399. https://doi.org/10.1016/j.gecco.2024.e03399
30. Weng, E.S., *et al*. „ Predicting Vegetation Types Using Leaf Traits and Their Physiological–Environmental Interactions: Insights From Evergreen and Deciduous Forests in an Earth System Modeling Framework.“ *Global Change Biology,* vol. 23, no. 6, 2017, pp. 2482–2498. https://doi.org/10.1111/gcb.13542
31. Magyar, T., *et al*. „ Improvement of N and P Ratio for Enhanced Biomass Productivity and Sustainable Cultivation of Chlorella vulgaris Microalgae.“ *Heliyon*, vol. 10, 2024, p. e23238. https://doi.org/10.1016/j.heliyon.2023.e23238
32. Sack, L. and C. Scoffoni. „Leaf Venation: Structure, Function, Development, Evolution, Ecology and Applications in the Past, Present and Future.“ *New Phytologist*, vol. 198, no. 4, 2013, pp. 983–1000. https://www.doi.org/10.1111/nph.12253
33. Poorter, H., et al. „A Meta-Analysis of Plant Responses to Light Intensity for 70 Traits Ranging from Molecules to Whole Plant Performance.“ *New Phytologist*, vol. 223, 2019, pp. 1073–1105. https://doi.org/10.1111/nph.15754
34. Cho, A., *et al*. „Leaf Functional Traits Highlight Phenotypic Variation of Two Tree Species in the Urban Environment.“ *Frontiers in Plant Science*, vol. 15, 2024, p. e1450723. https://doi.org/10.3389/fpls.2024.1450723
35. Rötzer, T., *et al*. „Modelling Urban Tree Growth and Ecosystem Services: Review and Perspectives.“ *Progress in Botany*, vol. 82, 2021, pp. 405–464. https://doi.org/10.1007/124_2020_46
36. Roloff, A., *et al*. „The Climate-Species-Matrix to Select Tree Species for Urban Habitats Considering Climate Change.“ *Urban Forestry & Urban Greening*, vol. 8, no. 4, 2009, pp. 295–308. https://doi.org/10.1016/j.ufug.2009.08.002
37. „Basic information of Zhengzhou city“. *Zhengzhou City Government*. https://www.zhengzhou.gov.cn/view4/index.jhtml Accessed 12 January 2025 (in Chinese)
38. Yuan, Q., *et al*. „Statistical Bias of Plant Functional Traits in Forest Ecosystems Caused by Different Classifications of Growth Form.“ *Acta Ecologica Sinica*, vol. 41, no. 3, 2021, pp. 1106–1115. http://doi.org/10.5846/stxb202002010188
39. Shaw, K. „Determination of Organic Carbon in Soil and Plant Material.“ *Journal of Soil Science*, vol. 10, no. 2, 1959, pp. 316–326. https://doi.org/10.1111/j.1365-2389.1959.tb02353.x
40. Wei, L., *et al*. „Above and Belowground Composition and Diversity of Subtropical Plantations and Their Relationships with Soil Nutrient Stocks.“ *Plant and Soil*, vol. 495, no. 1-2, 2024, pp. 235–252. https://doi.org/10.1007/s11104-023-06317-8
41. Schroeder A.B., *et al*. „The ImageJ ecosystem: Open-source software for image visualization, processing, and analysis.“ *Protein science*, vol. 30, no. 1, 2021, pp. 234–249. https://doi.org/10.1002/pro.3993
42. OriginLab. „Multivariate Analysis of Variance (MANOVA).“ *OriginLab*, OriginLab Corporation. https://www.originlab.com/doc/App/MANOVA. Accessed 18 Mar. 2025
43. Packard, G.C. „Is Logarithmic Transformation Necessary in Allometry?“ *Biological Journal of the Linnean Society*, vol. 109, no. 2, 2013, pp. 476–486. https://doi.org/10.1111/bij.12038
44. National Platform for Common GeoSpatial Information Services. „Tianditu (Map World).“ National Geomatics Center of China. https://www.tianditu.gov.cn. Accessed 1 Mar. 2025